

Response to N. Jakowski (Referee) (RC1)

Responses are included in line below in red.

The authors thank Dr Jakowski for his review and for this recommendation that our paper should be published.

We also note that Dr Jakowski refers to our statement that remaining kappa biases at nighttime can be ignored in practical applications due to the smallness of the consequent bending angle errors. He goes on with an interesting discussion on the possible reason for a residual nighttime bias and we agree that a likely cause is the difference in vertical profile shape between day and night. However, we would make three points:

1. The comment concerning the small bending angle errors at night refers to the scalar kappa value, not to the func-kappa. The functional kappa exhibits very little bias difference from day to night and the resultant bending angles errors can be seen to be reasonable symmetric about zero for day and night (fig17 and 18)
2. We have tried including an explicit dependency on local time in the model. It does not provide any additional model skill, suggesting that it does not do a better job of capturing the local time variability than the solar zenith angle.
3. It is important to remember that we are building our model by fitting kappa derived from NeQuick. NeQuick is based on the standard CCIR databases of foF2, foE and M3000F2, and therefore provides a reasonable median model of F and E regions' peaks. However, it is not certain that NeQuick is a good median representation of the layer shapes. Our approach, therefore, is to model kappa with minimal complexity to try to avoid a close fitting to NeQuick that may be inappropriate in reality. It would be fair to say that our results are indicative that a simple kappa model may be used, but that further testing with real data must be used to validate this. This will form the basis of a subsequent paper, but we have tried to be clearer in this point in the discussion section.

Technical corrections:

P6, 119: there is only one subsection, therefore should be cancelled
There was an error in the section numbering. This has been corrected

P6 equation 8: the term dh looks like an increment of h, perhaps the coefficient symbol could be changed
Agreed. Changed to "e"

P9, 14: GPS instead of Gps
Agreed. Now changed

Figure 9: unit of kappa missing
Agreed. Now added

Figures 8, 10-15: Axis font size too small
Agreed. Increased size

Response to Anonymous review (RC3)

Responses are included in line below in red.

The authors consider residual error of the standard ionospheric correction, linear combination of L1 and L2 bending angles, related to ray separation at L1 and L2 GPS frequencies. In previous publications, this second order effect was approximated by squared L1-L2 bending angle with the coefficient. In the reviewed paper, the authors come up with the global model of the fitting coefficient and demonstrate that such model results in more effective reduction of the residual ionospheric error than constant coefficient. The results may be useful for climate applications of the GPS RO. I recommend publishing the paper after revision with account for comments below.

The authors thank the reviewer for her helpful comments and her recommendation to publish.

In this study, the authors: (i) assume local spherical symmetry of electron density; (ii) neglect higher order terms in the Appleton-Hartree equation. It may be useful to introduce these approximations at the beginning of the paper (currently (i) is mentioned in the last sentence of conclusions, while (ii) is not mentioned). Also, it may be useful to include reference to the paper by Hardy et al. (this paper may be available from different sources, see information at the end of the review). The paper by Hardy et al. also includes references to earlier publications on the second order ionospheric effects.

Agreed.

Reference to Hardy has been included. The following sentences have also been added to section 2:

“Horizontal gradients will result in residual errors in the inversion. However, it is expected that these errors are random; therefore, they should not affect monthly or seasonal climatologies.”

“The first order approximation neglects terms involving higher powers of the frequency and the earth’s magnetic field; however these have little effect on the residual bending angle errors (Syndergaard 2000).”

p.1, lines 13-14; p.5, lines 13-14: *"The main area of interest for k estimation is between 40 and 80 km. It is in this region where the residual error from the ionospheric correction is likely to be a major contributor to the overall error budget of neutral atmosphere retrievals."*

First, why 40-80 km is the region of interest? I believe that for weather and climate applications, GPS RO may be somewhat useful at 40 km but it is totally useless at 80 km. An explanation or reference is needed. Second, "likely" means the authors are not sure that large-scale ionospheric residual is the major error contributor. An explanation or reference would be helpful.

A more detailed description of the useful vertical limits of k has been included in section 3.2

p.1, line 13: *"As expected, the residual bending angle is well correlated (negatively) with the vertical TEC. However, k is more strongly dependent on the solar zenith angle."* In the context of the first sentence, the second sentence is not clear. In the approximation used by the authors, k depends only on electron density. The electron density, in turn, depends on the solar zenith

angle. Thus k depends on the solar zenith angle through the electron density, and the expression "more strongly dependent" is not clear, unless it is explained "more strongly than what (?)". Also, see comment to p.5, line 24.

We agree that this was unclear. The point is that whilst the residual bending angle error is strongly related to the TEC, the k is more strongly related to the solar zenith angle. This indicates that the TEC dependent component of the residual error is largely modelled effectively by the squared L1/L2 bending angle difference term in the correction. Thus, the k term is capturing other features such as the hmF2 variability. We have updated the text to make this clearer.

p.1, lines 16-17: "*The global mean error (i.e. bias) and the standard deviation of the residual errors are reduced to -2.2×10^{-10} rad and 2.0×10^{-9} rad respectively.*" First, the number to which something is reduced requires the number from which that something is reduced. Second, it is not clear from the context, whether the reduction is relative to $k=0$ or $k=\text{const}$? The abstract should be self-explanatory. Also, see comment to p.7, line 12.

Agreed. Text has been amended to compare results of the uncorrected case to the model k case

p.2, line 17: "... *simple of implement* ..." It should be "simple to implement".

Agreed. Text amended

p.2, line 22: "*Examples of now k varies with height* ..." It should be "how" instead of "now".

Agreed. Text amended

p.3, line 1: " r_t " is introduced but never used. Is it needed?

This is the lower limit in the equation 1 integral, so should be defined.

p.3, lines 14-15: "... *bending angle error ... which increases as a function of the electron density squared, integrated over the vertical profile.*" This sentence is not clear in several respects. First, it is said "increases", but not said with what parameter? "Increases as a function" does not make sense (function may increase or decrease). Second, "integration over" is commonly used with respect to domain (e.g., over height interval). Integration "over the profile" is not a common expression. Third, if the authors mean equation (22) from VK94, it is more complicated than just integrated squared electron density; it includes derivative and kernel. This sentence should be made clear and reference provided.

We agree that this was unclear. We have amended the text to read:
"One downside is that a systematic bending angle error remains (see equation 5 of Healy & Culverwell 2015). The bending angle error has a dependence on the electron density squared,

which indicates that it will vary with the solar cycle. This has been recognised as a potential source of bias in climatology products (Danzer et al. 2013).”

p.3, line 24: "... *as a function of ... time ...*" Logically, it should be "local time".

Agreed. Text amended

p.4, line 2: "*A month median ...*" It should be "A monthly median".

Agreed. Text amended

p.4, line 10: "PRIME" and "COST 238" should be explained.

Agreed. Text amended.

p.4, line 12: "... *current version NeQuick ...*" It should be "current version of NeQuick".

Agreed. Text amended

p.4, line 13: "... *Galileo GNSS system ...*"
In the "GNSS", the last "S" already stands for "system". The expression above should be corrected and "GNSS" explained.

Agreed. Text amended

p.5, line 16: "*Example height dependence*" It should be "Example of height dependence"

Modified to “Height dependence” for consistency with the following sections

p.5, line 19: "... *k is approximately linear ...*" Linear with what parameter?

Tangent height. Text amended

p.5, line 24: "... *k appears to be more strongly dependent ...*"
More strongly than what? Also, see comment to p.1, line 13.

We agree that this was unclear. The point is that whilst the residual bending angle error is strongly related to the TEC, the k is more strongly related to the solar zenith angle. This indicates that the TEC dependent component of the residual error is largely modelled effectively by the squared L1/L2 bending angle difference term in the correction. Thus, the k term is capturing other features such as the hmF2 variability. We have updated the text to make this clearer:

“However, κ is more strongly dependent on the solar zenith angle, indicating that the TEC dependent component of the residual error is largely modelled by the squared L1/L2 bending angle difference term in the correction, and that κ is modelling other features such as changes in hmF2.”

p.5, lines 30-32: What is the physical sense of the statement that dynamic range of k is smaller than of F10.7? What are practical conclusions from this statement? This should be explained, otherwise I don't see why is this statement needed.

This is similar to the previous point. The reduction in dynamic range indicates that k is only weakly dependent on the electron density changes associated with the change in f10.7 through the solar cycle. We have added an explanatory sentence referring back to the previous section. “This, again, is indicative of the TEC dependent component of the residual error being largely modelled by the squared L1/L2 bending angle difference term in the correction.”

p.6, line 11: "*In order the build the models...*" It should be "in order to build the models".

Agreed. Text amended.

p.6, lines 20-25: It may be better to introduce " χ " here (rather than after equation 8) because " χ " is used in discussion of figures 11-13.

We do not think the symbol χ needs to be introduced until equation 8. However, to avoid any confusion, we have included the symbol in the captions of Figures 11-13.

p.6, lines 11-13; p.7, line 7: What is the reason for using two different sets, generated with the same "random drivers", for building and testing the k -model? I assume that the sets are statistically representative and the results are statistically significant. Will the results be substantially different with the use of one set for building and testing?

The aim is simply to have a statistically similar, but independent set of data for testing the models. Given the size of the test sets and the low complexity of the proposed model, we do not expect the model parameters to vary significantly if determined from one set or the other.

p.7, line 12: "... residual errors are reduced to 2.2×10^{-10} rad and 2.0×10^{-9} rad respectively." The number to which something is reduced requires the number from which that something is reduced. Also, see comment to p.1, lines 16-17.

Agreed. Text has been amended to compare results of the uncorrected case to the model k case

Figure 9: Axes labels on all figures, except Figure 9, have units in parentheses. Thus " k (impact parameter 60 km)" is confusing. It should be " k (1/rad)". The title above the figure can be changed to " k value at 60 km above London".

Agreed. Figure has been amended.

Figure 16: I think, "left" and "right" are mixed up in the caption. Left is full histogram, while right is zoomed to highlight tails.

Agreed. Text amended.

Improved model for correcting the ionospheric impact on bending angle in radio occultation measurements

Matthew J. Angling¹, Sean Elvidge¹, Sean B. Healy²

¹Space Environment and Radio Engineering Group, University of Birmingham, UK.

5 ²European Centre for Medium-range Weather Forecasts (ECMWF), Reading, UK.

Correspondence to: Matthew J. Angling (m.angling@bham.ac.uk)

Abstract. The standard approach to remove the effects of the ionosphere from neutral atmosphere GPS radio occultation measurements is to estimate a corrected bending angle from a combination of the L1 and L2 bending angles. This approach is known to result in systematic errors and an extension has been proposed to the standard ionospheric correction that is dependent on the squared L1/L2 bending angle difference and a scaling term (κ). The variation of κ with height, time, season, location and solar activity (i.e. the f10.7 flux) has been investigated by applying a 1D bending angle operator to electron density profiles provided by a monthly median ionospheric climatology model. As expected, the residual bending angle is well correlated (negatively) with the vertical TEC. However, κ is more strongly dependent on the solar zenith angle, indicating that the TEC dependent component of the residual error is effectively modelled by the squared L1/L2 bending angle difference term in the correction. The residual error from the ionospheric correction is likely to be a major contributor to the overall error budget of neutral atmosphere retrievals between 40-80 km. Furthermore, over this height range of interest (40-80 km) κ is approximately linear with height. A simple κ model has also been developed. It is independent of ionospheric measurements, but incorporates geophysical dependencies (i.e. solar zenith angle, solar flux, altitude). The global mean error (i.e. bias) and the standard deviation of the residual errors are reduced from -1.3×10^{-8} and 2.2×10^{-8} for the uncorrected case to -2.2×10^{-10} rad and 2.0×10^{-9} rad respectively for the corrections using the κ model. Although a fixed scalar κ also reduces bias for the global average the selected value of κ (14 rad^{-1}) is only appropriate for a small band of locations around the solar terminator. In the day time, the scalar κ is consistently too high and this results in an over correction of the bending angles and a positive bending angle bias. Similarly, in the night time, the scalar κ is too low. However, in this case, the bending angles are already small and the impact of the choice of κ is less pronounced.

25

1. Introduction

It has been demonstrated that, by using variational data assimilation techniques, GPS radio occultation (GPS-RO) measurements can be assimilated into operational numerical weather prediction (NWP) systems to improve the accuracy of temperatures in the upper troposphere and lower/middle stratosphere (Healy & Thépaut 2006; Poli et al. 2009; Rennie 2010). In particular, GPS-RO measurements reduce stratospheric temperature biases in NWP systems and this indicates that such measurements could have an increasingly important role in climate monitoring and climate reanalyses (Poli et al. 2010; Steiner et al. 2013). Notwithstanding the benefits of GPS-RO for the neutral atmosphere, it remains necessary to consider the effect of the ionosphere on the measurements.

35 Vorob'ev & Krasil'nikova (1994) (hereafter referred to as VK94) proposed a method of combining the GPS-RO bending angles measured at two frequencies (L1 and L2) to provide a first order correction for the ionosphere. VK94 also showed that the first order correction leaves a systematic bending angle bias that increases as a function of the electron density squared, integrated over the vertical profile. The relationship between the bias and electron density suggests that the bending angle

biases should vary diurnally and as a function of the 11-year solar cycle. This has been demonstrated by various authors; e.g. (Kursinski et al. 1997; Mannucci et al. 2011; Danzer et al. 2013).

Healy & Culverwell (2015) have proposed a modification to the standard bending-angle correction to reduce the residual systematic ionospheric errors. The modification introduces a new second-order term that is a function of the square of L1 and L2 bending angle difference and a weighting term (κ). The aim of this work is to investigate the variation of κ with height, time, season, location and solar activity (i.e. the f10.7 flux). This has been done by applying a 1D bending angle operator to electron density profiles provided by the NeQuick monthly median ionospheric climatology model (Nava et al. 2008). As well as examining the variations in κ , a κ model has been developed. It is independent of ionospheric measurements, and therefore simple to implement in an operational system, but does incorporate the relevant geophysical dependencies (i.e. solar zenith angle, solar flux). The expectation is that, since NeQuick is a reasonable median model of the ionosphere, the κ model derived from it will also exhibit reasonable statistics, though this has not been proven.

Radio occultations, the VK94 ionospheric correction procedure, and the proposed modified correction are described in Section 2. Examples of how κ varies with height, location and solar activity are presented in Section 3. Models for κ are proposed and assessed in Section 4 and the discussion and conclusions are given in Sections 5 and 6.

2. Radio occultation and ionospheric corrections

(Hardy et al. (1994), Kursinski et al. (1997) and Hajj et al. (2002) provide a comprehensive description of the GPS-RO technique. In summary, the GPS satellites transmit on two L-band channels (L1, L2) at $f_1 = 1575.42$ MHz and $f_2 = 1227.60$ MHz and the signals are received by a satellite in low earth orbit (LEO) (Figure 1).

The standard approach (Abel Transform) for inverting GPS-RO measurements requires the assumption of spherical symmetry. Assuming spherical symmetry Under that assumption, the bending angle of the ray between the GPS satellite and a receiver in LEO is:

$$\alpha_{Li}(a) = -2a \int_{r_t}^{\infty} \frac{dn_i/dr}{n_i \sqrt{(n_i r)^2 - a^2}} dr \quad \text{Equation 1}$$

where $i = 1,2$ depending on the frequency; a is the impact parameter; r_t is the tangent height of the ray path; and n_i is the refractive index. The impact parameter is given by:

$$a = nr \sin(\phi) = \text{const} \quad \text{Equation 2}$$

Horizontal gradients will result in residual errors in the inversion. However, it is expected that these errors are random; therefore, they should not affect monthly or seasonal climatologies.

To a first order approximation, the refractive index comprises terms dependent on the neutral atmosphere refractivity (N_n), the ionospheric electron density (n_e), and the frequency (f) squared:

$$n_i \cong 1 + 10^{-6} N_n(r) - k \frac{n_e(r)}{f_i^2} \quad \text{Equation 3}$$

where $k = 40.3 \text{ m}^3 \text{ s}^{-2}$. Therefore, the measured L1 and L2 bending angles are different from each other, and contain both neutral and ionospheric components. The standard approach taken in operational RO processing centres is to estimate a corrected neutral atmosphere bending angle (α_c) using the VK94 approach:

$$\alpha_c(a) = \alpha_{L1}(a) + \frac{f_2^2}{f_1^2 - f_2^2} [\alpha_{L1}(a) - \alpha_{L2}(a)] \quad \text{Equation 4}$$

where the L1 and L2 bending angles (α_{L1} and α_{L2} respectively) are interpolated to a common impact parameter. The first order approximation neglects terms involving higher powers of the frequency and the earth's magnetic field; however these have little effect on the residual bending angle errors (Syndergaard 2000). One benefit of this approach is that it is based on the standard parameters estimated by the RO retrieval system and does not require *a priori* information about the ionosphere. One downside is that a systematic bending angle error remains (see equation 5 of Healy & Culverwell 2015). The bending angle error has a dependence on which increases as a function of the electron density squared, which indicates that it will be integrated over the vertical profile. These residual ionospheric errors vary with the solar cycle. This and hasve been recognised as a potential source of bias in climatology products (Danzer et al. 2013). Healy & Culverwell (2015) have proposed a modification to the standard ionospheric correction of the form:

$$\alpha_c(a) = \alpha_{L1}(a) + \frac{f_2^2}{f_1^2 - f_2^2} [\alpha_{L1}(a) - \alpha_{L2}(a)] + \kappa(a)(\alpha_{L1}(a) - \alpha_{L2}(a))^2 \quad \text{Equation 5}$$

where the κ term compensates for the systematic residual error in the standard approach. An appropriate value for κ has been investigated using simple analytic functions for the ionosphere (Healy & Culverwell 2015) and using a raytracer through a 3D ionospheric model (Danzer et al. 2015), though it should be noted that this study was limited to a low latitude band because of noise in the simulation system. It has been shown that κ generally falls in the range of 10 to 20 rad^{-1} and a simple scalar model, $\kappa \sim 14$, provides a good first approximation, improving the accuracy of the “dry” temperature retrievals (Danzer et al. 2015). Nevertheless, it is clear that κ will vary as a function of height, local time, season, location and solar activity and therefore it is possible that existing ionospheric climatology models could be used to compute an improved correction term by modelling the monthly mean, temporal and spatial variations of κ more realistically.

3. Examples of κ dependencies

A monthly median 3D ionospheric model (in this case NeQuick) and a 1D bending angle operator (based on Equation 1) can be used to estimate the residual ionospheric error and thereby estimate values for κ .

3.1. NeQuick

NeQuick is a monthly median ionospheric electron density model developed at the Aeronomy and Radiopropagation Laboratory (now Telecommunications/ICT for Development Laboratory) of the Abdus Salam International Centre for Theoretical Physics (ICTP), Trieste, Italy, and at the Institute for Geophysics, Astrophysics and Meteorology (IGAM) of the University of Graz, Austria (Nava et al. 2008). The model is based on the Di Giovanni - Radicella (DGR) model (Di Giovanni & Radicella 1990) which was modified for the European Cooperation in Science and Technology (COST) Action PRIME project in COST 238 to provide electron densities from ground to 1000 km. The model has been designed to have continuously integrable vertical profiles which allows for rapid calculation of the TEC for trans-ionospheric propagation applications. The current version of NeQuick can be run up to a height of 20000 km and is used in the Galileo global navigation satellite system (GNSS) system to calculate ionospheric corrections (Angrisano et al. 2013).

NeQuick is a "profiler" which makes use of three profile anchor points at the E layer peak, the F1 peak, and the F2 peak. To specify the anchor points it uses the layer critical frequencies (f_oE , f_oF1 , f_oF2) and the F2 maximum usable frequency factor

(M3000(F2)) (Davies 1965). foE is determined using a solar zenith angle model; foF1 is assumed to be proportional to foE during daytime and zero during nighttime; and foF2 and M3000(F2) are derived from the ITU-R (CCIR) coefficients in the same way as the International Reference Ionosphere (IRI) (Bilitza & Reinisch 2008).

- 5 Between 100 km and the peak of the F2 layer, NeQuick uses an electron density profile based on the superposition of five semi-Epstein layers (Epstein 1930; Rawer 1983); i.e. the Epstein layers have different thickness parameters for their top and bottom sides. The topside of NeQuick is a simplified approximation to a diffusive equilibrium. A semi-Epstein layer represents the model topside with a height-dependent thickness parameter that has been empirically determined.
- 10 The model used in this work is the University of Birmingham’s translation of the NeQuick v2.0.2 from FORTRAN into Python. Very minor (negligible) differences in results are observed due to the use of different interpolation routines. The Python code has been largely vectorised to increase the speed of operation. Some additional modifications have been made and are described in [Table 1](#).

15 3.2. κ estimation

In each of the examples shown in the following sections the same basic procedure has been followed to estimate the value of κ :

1. Use NeQuick to estimate a vertical profile of electron density
2. Convert the electron density (n_e), to the refractive index (n_i) using the 1st order approximation ($n_i = 1 - 40.3n_e/f_i^2$)
20 for each frequency (L1 and L2)
3. Estimate bending angle using the 1D observation operator for L1 and L2
4. Form the VK94 corrected bending angle (α_c).

Since no neutral atmosphere is included in the estimate of the refractive index, α_c should be zero if VK94 provides a perfect correction. Any non-zero values are representative of the residual ionospheric error ($\Delta\alpha$) which, from [Equation 5](#), is
25 modelled as:

$$\Delta\alpha = \kappa(a)(\alpha_{L1}(a) - \alpha_{L2}(a))^2 \quad \text{Equation 6}$$

Since the bending angles are known, this can be rearranged to provide an estimate of κ as a function of the impact parameter:

$$\kappa(a) = \frac{\Delta\alpha}{(\alpha_{L1}(a) - \alpha_{L2}(a))^2} \quad \text{Equation 7}$$

30 [In real data the corrected bending angles increase rapidly towards the surface. This means that the impact of any residual error becomes less insignificant below approximately 40 km. Furthermore, the VK94 correction assumes that the ray impact parameter/tangent height is below the ionosphere \(i.e. the electron density is zero\). Consequently,](#) The main area of interest for κ estimation is between 40 and 80 km. It is in this region where the residual error from the ionospheric correction is likely
35 to be a major contributor to the overall error budget of neutral atmosphere retrievals.

3.3. [Example h](#)Height dependence

The Figure 2 to Figure 5 show two examples of the vertical electron density profile, the L1/L2 bending angles, the residual error and κ . The test parameters are given in [Table 2](#). Over the height range of interest (40-80 km), Figure 5 shows that
40 κ is approximately linear [with tangent height](#), but its gradient is dependent on the local time.

3.4. Geographic dependence

The geographic dependence of bending angle correction can be demonstrated by plotting maps of the TEC (Figure 6), residual bending angle (Figure 7) and κ (Figure 8). In this case, the test parameters are given in Table 3. As expected, the residual bending angle is well correlated (negatively) with the vertical TEC. However, κ appears to be more strongly dependent on the solar zenith angle, indicating that the TEC dependent component of the residual error is largely modelled by the squared L1/L2 bending angle difference term in the correction, and that κ is modelling other features such as changes in hmF2.

3.5. Solar cycle dependence

The solar cycle dependence of κ has been investigated by estimating κ at a tangent height of 60 km above London for each day over the last 60 years (Table 4). The results (Figure 9) show that κ is negatively correlated with f10.7; i.e. κ is low when the vertical TEC is large which occurs when f10.7 is high. Furthermore, the dynamic range of κ is considerably smaller than that of the f10.7 (and hence TEC and bending angle), varying by a factor of approximately 50% compared to approximately 300% for f10.7. This, again, is indicative of the TEC dependent component of the residual error being largely modelled by the squared L1/L2 bending angle difference term in the correction.

4. Models of κ

4.1. Introduction

Section 3 has presented examples of how κ can vary spatially and with solar cycle. In this section, simple models of κ will be assessed in order to evaluate their potential to reduce the residual bending angle errors in the VK94 correction. Three models will be considered:

- κ equals zero (zero- κ); this represents the current situation with the unmodified VK94 correction
- κ is a scalar (scal- κ); this is the approach proposed by Healy & Culverwell (2015)
- κ is a function of latitude, longitude, solar zenith angle and solar flux (func- κ).

In order to build the models a set of 25000 κ estimates were generated from NeQuick using random drivers (uniformly distributed over the ranges in Table 5). The true solar flux is used for each randomly selected day/year. A further independent set of 25000 κ estimates were also generated using the same random parameter ranges to act as a test data set.

4.2. Scalar κ

The random κ values are shown in Figure 10. The median value is marked by the horizontal line and has value of 14 rad⁻¹. This value is used as the scalar model.

4.3. Functional form κ

The aim of this model is to produce a very simple polynomial function that mimics some of the form of κ that is not accounted for by the scalar model. Figure 8 is suggestive that κ is a function of solar zenith angle – this is a convenient parameter to use since it embodies the position, local time and season. Figure 11, Figure 12 and Figure 13 show κ as a function of solar zenith angle, f10.7 and altitude respectively. Note that the solar zenith angle has been extended to π radians to account for when the sun is below the horizon. The figures indicate broadly linear dependencies in all cases; therefore, the following model is proposed:

$$\kappa = a + bf_{10.7} + c\chi + eh \quad \text{Equation 8}$$

Where $f_{10.7}$ is the f10.7 flux (sfu), χ is the solar zenith angle (rad) and h is the height above the ground (km); a, b, c, e are scalars to be found by fitting the model to the data.

The Python code `curve_fit` from the `scipy.optimize` package has been used to fit the model. The parameter results and the associated variances are shown in [Table 6](#). A plot of the NeQuick estimated κ compared to the func- κ is shown in [Figure 14](#). [Figure 15](#) shows the geographic distribution of func- κ at 12 UT in June and December at 60 km altitude and with an f10.7 of 150. These maps can be directly compared with those in [Figure 8](#).

4.4. Bending angle error reduction

The second set of 25000 randomly distributed points has been used to assess the reduction in residual bending angle for each of the κ models (zero- κ , scal- κ and func- κ). [Figure 16](#) shows a histogram of the residual bending angle errors for the full data set. The bending angle error statistics are in [Table 7](#).

Both the scal- κ and func- κ results are an improvement over the zero- κ results. In the case of the scal- κ , both the standard deviation and the mean error (i.e. bias) of the residual bending angle errors are reduced by an order of magnitude compared to the zero- κ results ([from \$-1.3 \times 10^{-8}\$ and \$2.2 \times 10^{-8}\$ for the zero- \$\kappa\$ case](#) to 5.4×10^{-9} rad and 1.5×10^{-9} rad, respectively, [Table 7](#)). In the case of the func- κ , the standard deviation and the mean error (i.e. bias) of the residual bending angle errors are further reduced to 2.0×10^{-9} rad and -2.2×10^{-10} rad respectively. Although the scal- κ reduces bias for the global average, the geographic variation of κ (shown in [Figure 8](#) and [Figure 15](#)) makes it clear that the selected value of κ (14 rad^{-1}) is, in fact, only appropriate for a small band of locations around the solar terminator. The effect of this is clear if the residual error statistics are considered for day time and night time separately.

[Figure 17](#) and [Figure 18](#) show histograms for residual bending angle for day and night respectively. In the day time, the scal- κ is consistently too high and this results in an over correction of the bending angles and a positive bending angle bias ([Table 7](#)). Similarly, in the night time, scal- κ is too low and this results in a negative bending angle bias. However, in this case, the bending angles are already small and the impact of the choice of κ is less pronounced ([Table 7](#)). Conversely, the func- κ results in a negative bending angle bias in the daytime and positive bias at night. In both cases, the bending angle biases are significantly lower than those produced with scal- κ .

5. Discussion

Many studies of ionospheric refraction of trans-ionospheric radio waves have shown that, in addition to the level of ionization, the shape of the vertical electron density profile plays a significant role; e.g. (Jakowski et al. 1994) and (Hoque & Jakowski 2008; Hoque & Jakowski 2010). It is important to remember that the functional model of κ has been created by fitting κ derived from NeQuick. NeQuick is based on the standard CCIR databases of foF2, foE and M3000F2, and therefore provides a reasonable median model of the F and E regions' peaks; however, it is not certain that NeQuick is a good median representation of the layer shapes. Furthermore, the κ model is derived from 1D estimates of the bending angle and so does not take non-spherical structures into consideration. The approach, therefore, has been to model kappa with minimal complexity to avoid a close fitting to NeQuick that may be inappropriate in reality. Additional terms have been also trialled in the model (such as local time), but these have not shown any significant improvement of the model presented in this paper. Given the limitation of the ionospheric model and the bending angle estimation, the results are indicative that a simple kappa model may be used, but that further testing with real data must be used to validate this.

6. Conclusions

Using the random selection of vertical profiles from the NeQuick the median κ has been shown to be 14 rad^{-1} and this is therefore an appropriate value for κ if it is to be represented by a single scalar. This value agrees well with the result from Healy & Culverwell (2015) and is in the range suggested by Danzer et al. (2015). Representing κ as a scalar has the advantage of simplicity and is appropriate if climate re-processing centres are focused on ensuring that global average biases are removed. However, it has been demonstrated that such an approach can lead to significant differences in the residual bending angle bias between day and night. In the day, the results indicate that the bending angle bias switches sign from $-3.3 \times 10^{-8} \text{ rad}$ for no correction, to $+7.6 \times 10^{-9} \text{ rad}$ for the scalar κ correction.

10

This limitation can be overcome using the simple κ function model. This approach does not require independent ionospheric measurements and so remains easy to implement. It should be noted that the κ model is based on a monthly median ionospheric model. Whilst this is a starting point it will be necessary to work with climate re-processing centres to develop an effective validation strategies of the bending angle corrections. It would also be useful to assess the sensitivity of stratospheric climatologies to the bending angle bias and standard deviation bounds determined by this study. Furthermore, the magnitude of other error terms (i.e. non-symmetry (Zeng et al. 2016)) should be assessed in light of these results.

15

7. Acknowledgements

This work was undertaken as part of a visiting scientist study funded by the Radio Occultation Meteorology Satellite Application Facility (ROM SAF) which is a decentralised processing center under the European Organisation for the Exploitation of Meteorological Satellites (EUMETSAT). The original NeQuick Fortran code was provided by ITCP.

20

8. References

Angrisano, A. et al., 2013. Benefit of the NeQuick Galileo Version in GNSS Single-Point Positioning. *International Journal of Navigation and Observation*, 2013, pp.1–11.

25

Bilitza, D. & Reinisch, B.W., 2008. International Reference Ionosphere 2007: Improvements and new parameters. *J. Adv. Space Res.*, 42(4), pp.599–609.

Chu, Y.-H., Wu, K.-H. & Su, C.-L., 2009. A new aspect of ionospheric E region electron density morphology. *Journal of Geophysical Research*, 114(A12), p.A12314. Available at: <http://doi.wiley.com/10.1029/2008JA014022>.

30

Danzer, J., Healy, S.B. & Culverwell, I.D., 2015. A simulation study with a new residual ionospheric error model for GPS radio occultation climatologies. *Atmos. Meas. Tech*, 8, pp.3395–3404. Available at: www.atmos-meas-tech.net/8/3395/2015/.

Danzer, J., Scherllin-Pirscher, B. & Foelsche, U., 2013. Systematic residual ionospheric errors in radio occultation data and a potential way to minimize them. *Atmospheric Measurement Techniques*, 6(8), pp.2169–2179. Available at: <http://www.atmos-meas-tech.net/6/2169/2013/amt-6-2169-2013.html> [Accessed November 29, 2016].

35

Davies, K., 1965. *Ionospheric radio propagation*, National Bureau of Standards, USA.

Epstein, P.S., 1930. Reflection of Waves in an Inhomogeneous Absorbing Medium. *Proceedings of the National Academy of*

- Di Giovanni, G. & Radicella, S.M., 1990. An analytical model of the electron density profile in the ionosphere. *Advances in Space Research*, 10(11), pp.27–30. Available at: <http://linkinghub.elsevier.com/retrieve/pii/027311779090301F> [Accessed August 8, 2016].
- 5 Hajj, G.A. et al., 2002. A Technical Description of Atmospheric Sounding By GPS. *J. Atmos. and Solar-Terr Phys.*, 64, pp.451–469.
- Hardy, K.R., Hajj, G.A. & Kursinski, E.R., 1994. Accuracies of atmospheric profiles obtained from GPS occultations. *International Journal of Satellite Communications*, 12(5), pp.463–473. Available at: <http://doi.wiley.com/10.1002/sat.4600120508> [Accessed December 8, 2017].
- 10 Healy, S.B., 2001. Radio occultation bending angle and impact parameter errors caused by horizontal refractive index gradients in the troposphere: a simulation study. *JGR*, 106(D11), pp.11875–11889.
- Healy, S.B. & Culverwell, I.D., 2015. A modification to the standard ionospheric correction method used in GPS radio occultation. *Atmospheric Measurement Techniques*, 8(8), pp.3385–3393. Available at: <http://www.atmos-meas-tech.net/8/3385/2015/>.
- 15 Healy, S.B. & Thépaut, J.-N., 2006. Assimilation experiments with CHAMP GPS radio occultation measurements. *Quarterly Journal of the Royal Meteorological Society*, 132(615), pp.605–623. Available at: <http://doi.wiley.com/10.1256/qj.04.182> [Accessed April 25, 2017].
- Hoque, M.M. & Jakowski, N., 2008. Estimate of higher order ionospheric errors in GNSS positioning. *Radio Science*, 43(5). Available at: <http://doi.wiley.com/10.1029/2007RS003817> [Accessed October 16, 2017].
- 20 Hoque, M.M. & Jakowski, N., 2010. Higher order ionospheric propagation effects on GPS radio occultation signals. *Advances in Space Research*, 46(2), pp.162–173. Available at: <http://www.sciencedirect.com/science/article/pii/S0273117710001183> [Accessed October 16, 2017].
- Jakowski, N., Porsch, F. & Mayer, G., 1994. Ionosphere-Induced Ray-Path Bending Effects in Precision Satellite Positioning Systems. *Zeitschrift f. satellitengestützte Positionierung, Navigation und Kommunikation SPN*, (1), pp.6–13. Available at: <http://elib.dlr.de/23702/> [Accessed October 16, 2017].
- 25 Kursinski, E.R. et al., 1997. Observing Earth’s atmosphere with radio occultation measurements using the Global Positioning System. *Journal of Geophysical Research*, 102(D19), pp.23429–23465.
- Mannucci, A.J. et al., 2011. The impact of large scale ionospheric structure on radio occultation retrievals. *Atmospheric Measurement Techniques*, 4(12), pp.2837–2850. Available at: <http://www.atmos-meas-tech.net/4/2837/2011/> [Accessed April 26, 2017].
- 30 Nava, B., Coisson, P. & Radicella, S., 2008. A new version of the neQuick ionosphere electron density model. *Journal of Atmos. and Solar-Terr. Physics*.
- Poli, P. et al., 2009. Quality Control, Error Analysis, and Impact Assessment of FORMOSAT-3/COSMIC in Numerical Weather Prediction. *Terrestrial, Atmospheric and Oceanic Sciences*, 20(1), p.101. Available at: <http://tao.cgu.org.tw/index.php/articles/archive/space-science/item/817> [Accessed April 25, 2017].
- 35 Poli, P., Healy, S.B. & Dee, D.P., 2010. Assimilation of Global Positioning System radio occultation data in the ECMWF ERA-Interim reanalysis. *Quarterly Journal of the Royal Meteorological Society*, 136(653), pp.1972–1990. Available at: <http://doi.wiley.com/10.1002/qj.722> [Accessed April 25, 2017].

Rawer, K., 1983. Replacement of the Present Sub-Peark Plasma Density Profile by a Unique Expression. *Advances in Space Research*, 2(10), pp.183–190.

Rennie, M.P., 2010. The impact of GPS radio occultation assimilation at the Met Office. *Quarterly Journal of the Royal Meteorological Society*, 136(646), pp.116–131. Available at: <http://doi.wiley.com/10.1002/qj.521> [Accessed April 25, 2017].

5

Steiner, A.K. et al., 2013. Quantification of structural uncertainty in climate data records from GPS radio occultation. *Atmospheric Chemistry and Physics*, 13(3), pp.1469–1484. Available at: <http://www.atmos-chem-phys.net/13/1469/2013/> [Accessed April 25, 2017].

Syndergaard, S., 2000. On the ionosphere calibration in GPS radio occultation measurements. *Radio Science*, 35(3), pp.865–883. Available at: <http://doi.wiley.com/10.1029/1999RS002199> [Accessed December 8, 2017].

10

Vorob'ev, V. V & Krasil'nikova, T.G., 1994. Estimation of the accuracy of the atmospheric refractive index recovery from the NAVSTAR system. *USSR Physics of the Atmosphere and Ocean (Eng. Trans.)*, 29(5), pp.602–609.

Zeng, Z. et al., 2016. Ionospheric correction of GPS radio occultation data in the troposphere. *Atmospheric Measurement Techniques*, 9(2), pp.335–346. Available at: <http://www.atmos-meas-tech.net/9/335/2016/>.

15

Figures

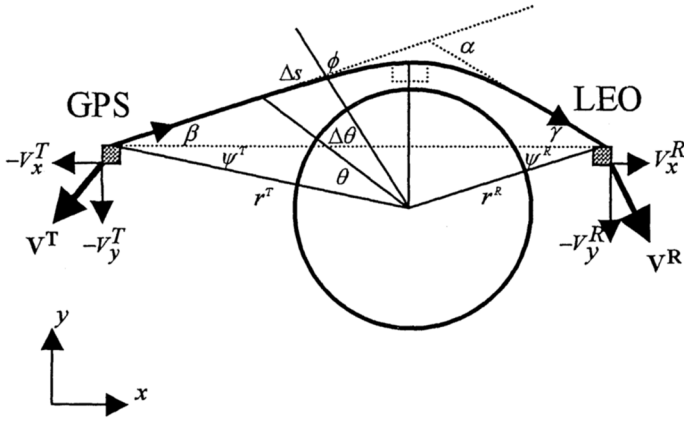
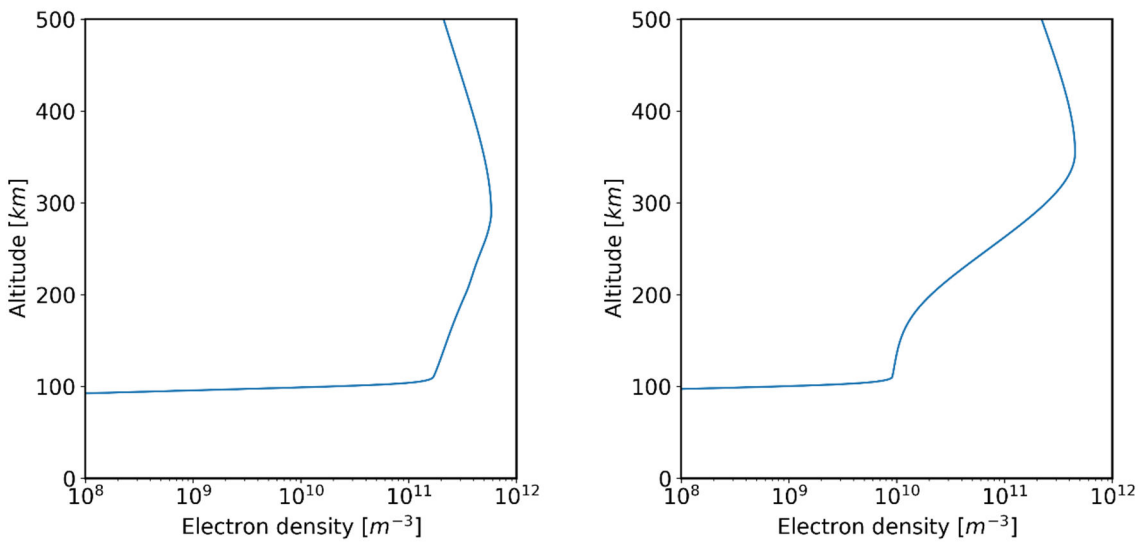


Figure 1: Radio occultation geometry. Reproduced from (Healy 2001)



5
Figure 2. Electron density profiles for test 1 (left, midday) and test 2 (right, midnight)

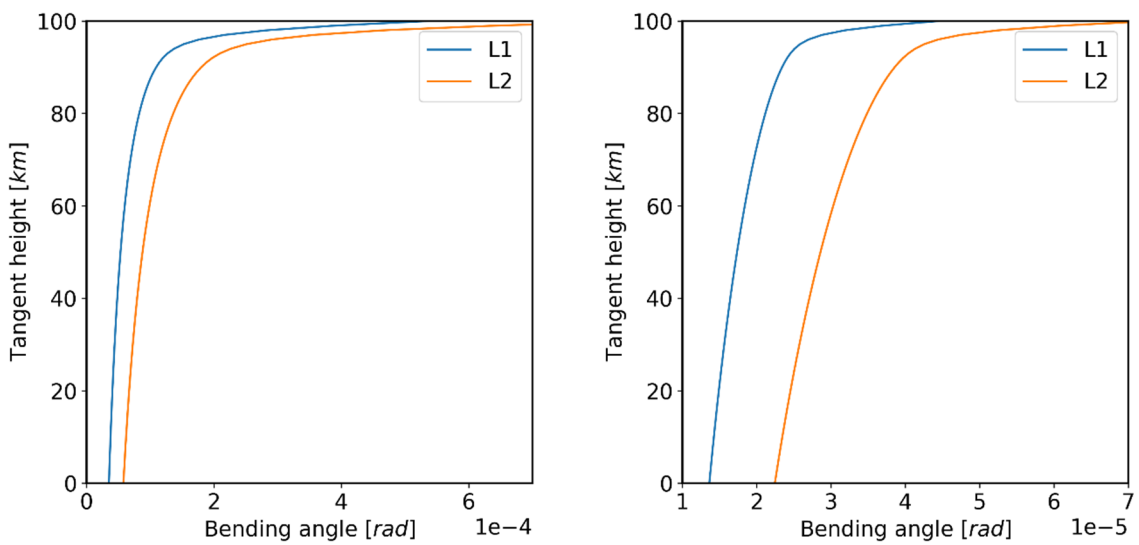


Figure 3. L1 and L2 bending angles for test 1 (left, midday) and test 2 (right, midnight)

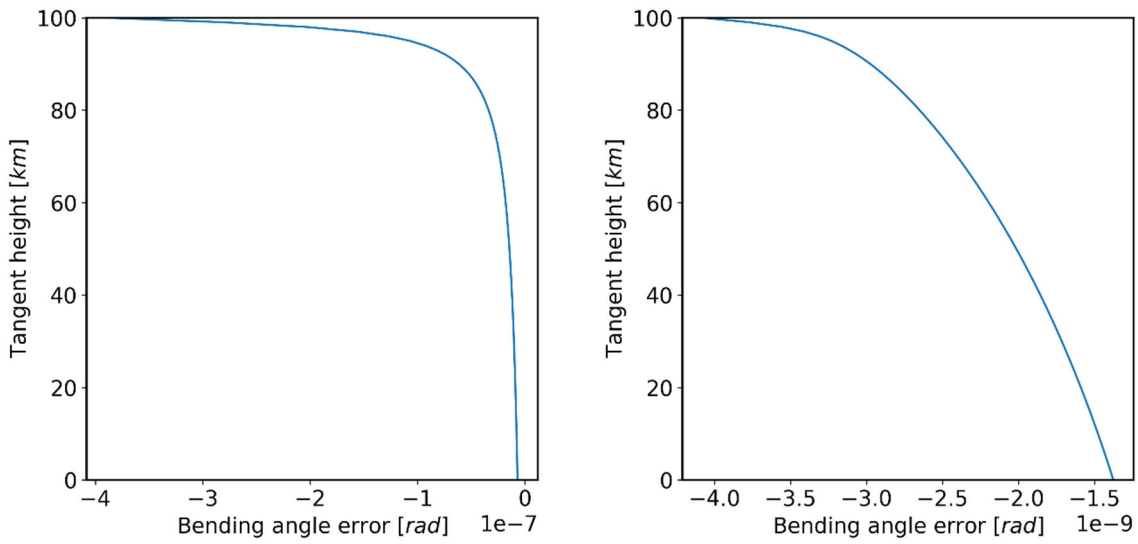
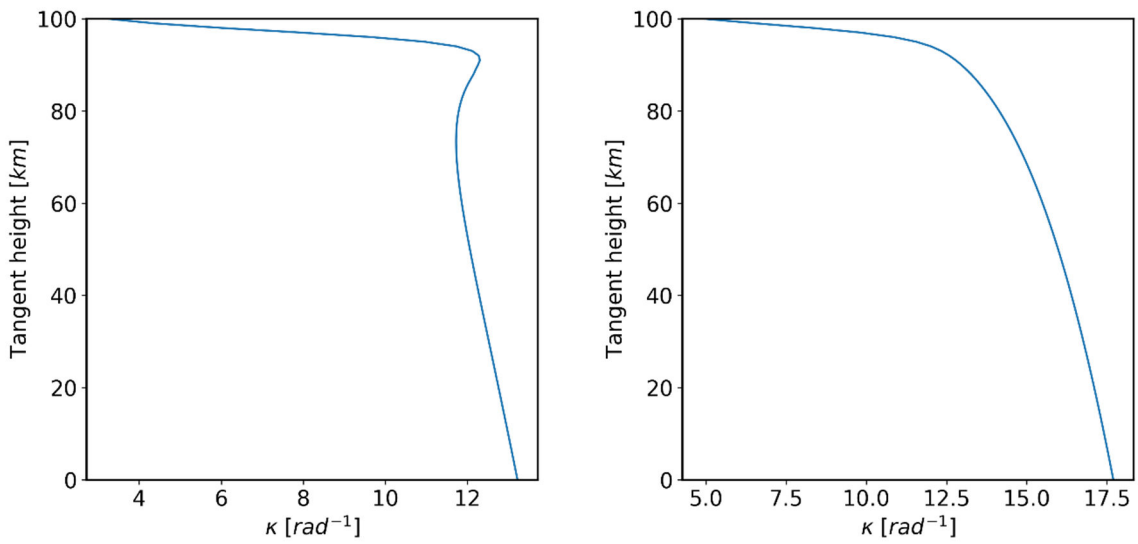


Figure 4. Bending angle residual errors for test 1 (left, midday) and test 2 (right, midnight)



5 Figure 5. Estimate of κ for test 1 (left, midday) and test 2 (right, midnight)

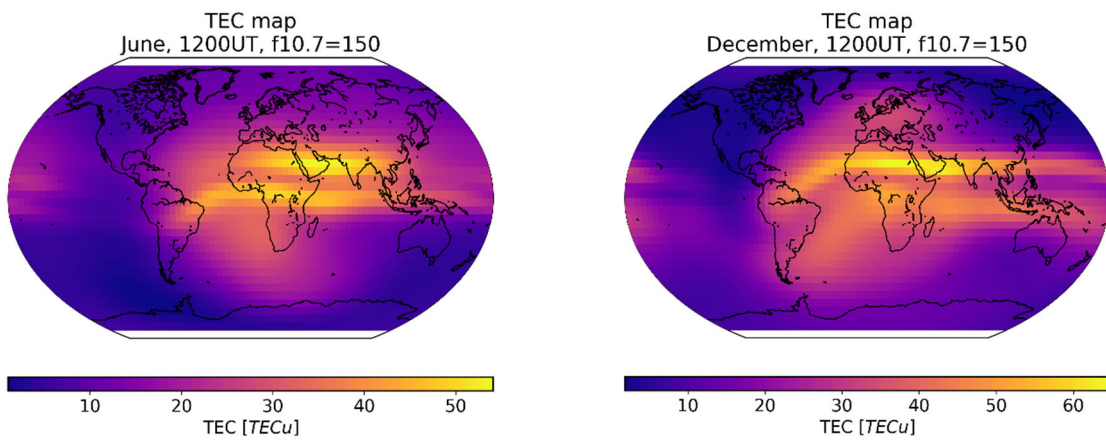
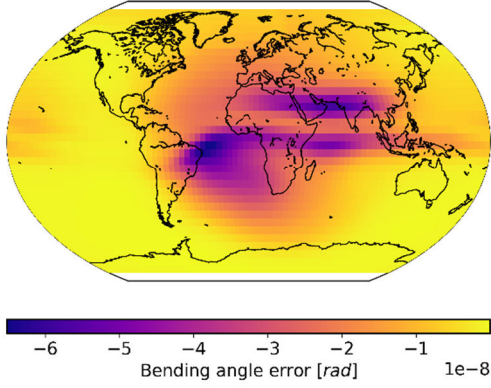


Figure 6. Vertical TEC from NeQuick for 12 UT, f10.7=150, June (left) and December (right).

Bending angle error map (tangent height 60km)
June, 1200UT, f10.7=150



Bending angle error map (tangent height 60km)
December, 1200UT, f10.7=150

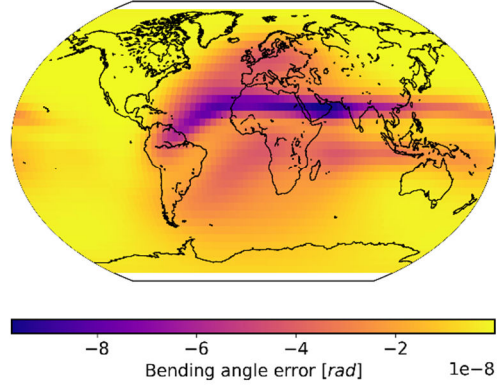
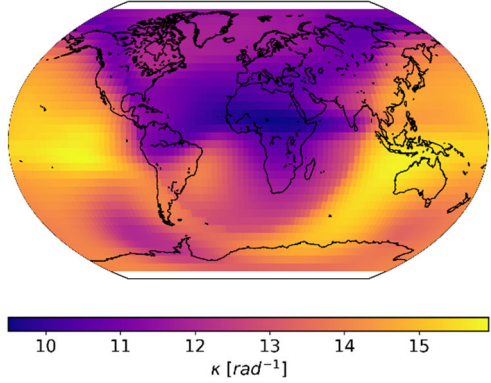
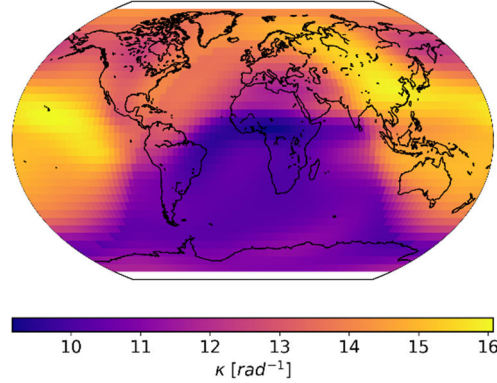


Figure 7. Estimated residual bending angle error for 12 UT, f10.7=150, June (left) and December (right).

κ map (tangent height 60km)
June, 1200UT, f10.7=150



κ map (tangent height 60km)
December, 1200UT, f10.7=150



5 Figure 8. Estimated κ for 12 UT, f10.7=150, June (left) and December (right).

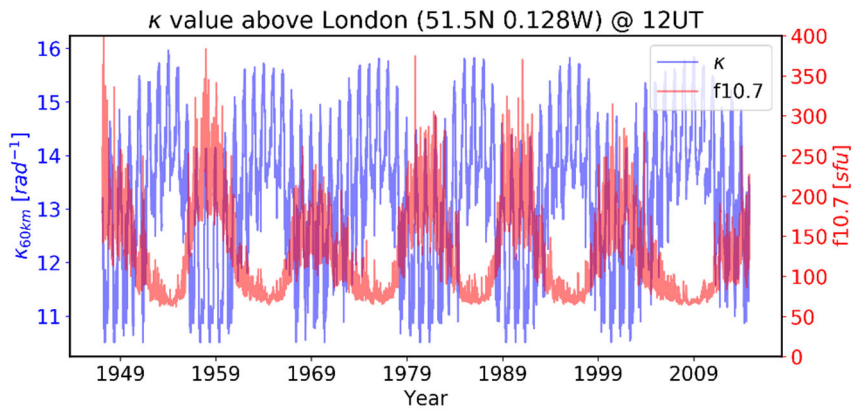


Figure 9. Solar cycle dependence of κ for a fixed location (London), tangent height (60 km) and local time (12UT).

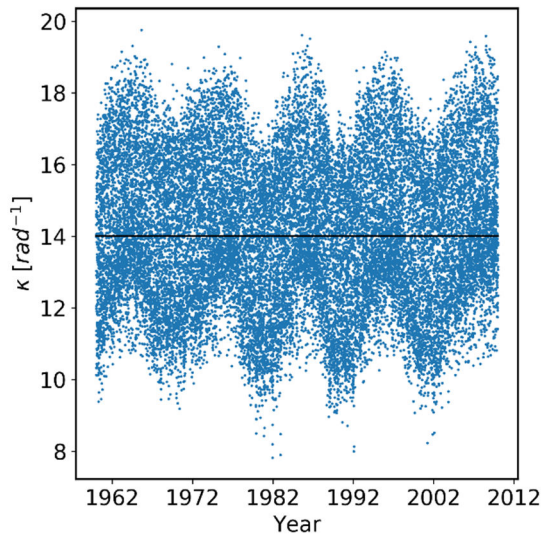
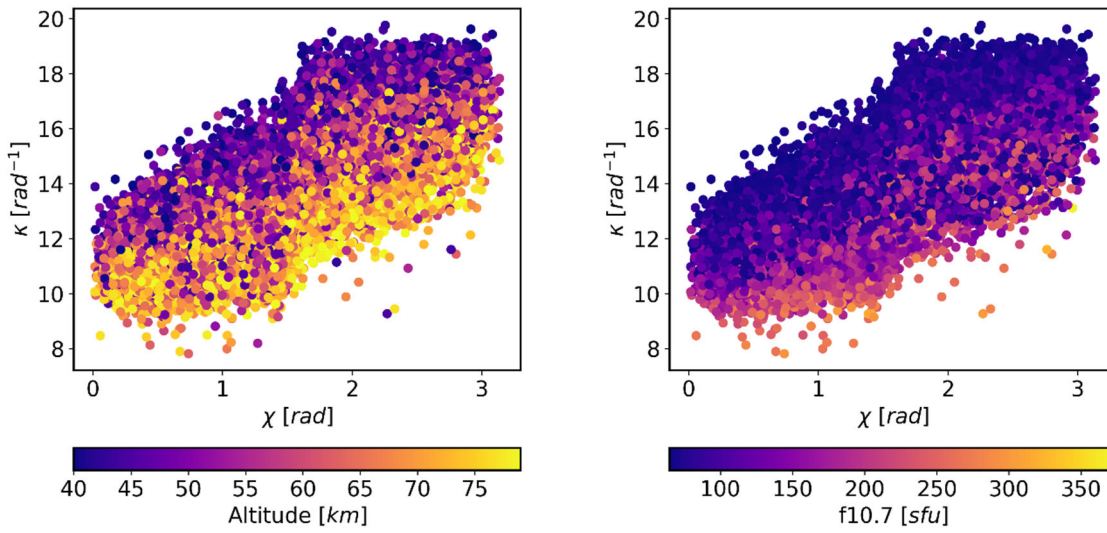


Figure 10. κ values for a random set of 25000 locations/times. The horizontal line marks the median ($=14 \text{ rad}^{-1}$).



5 Figure 11. κ vs. solar zenith angle (χ), colour coded by altitude (left) and f10.7 (right).

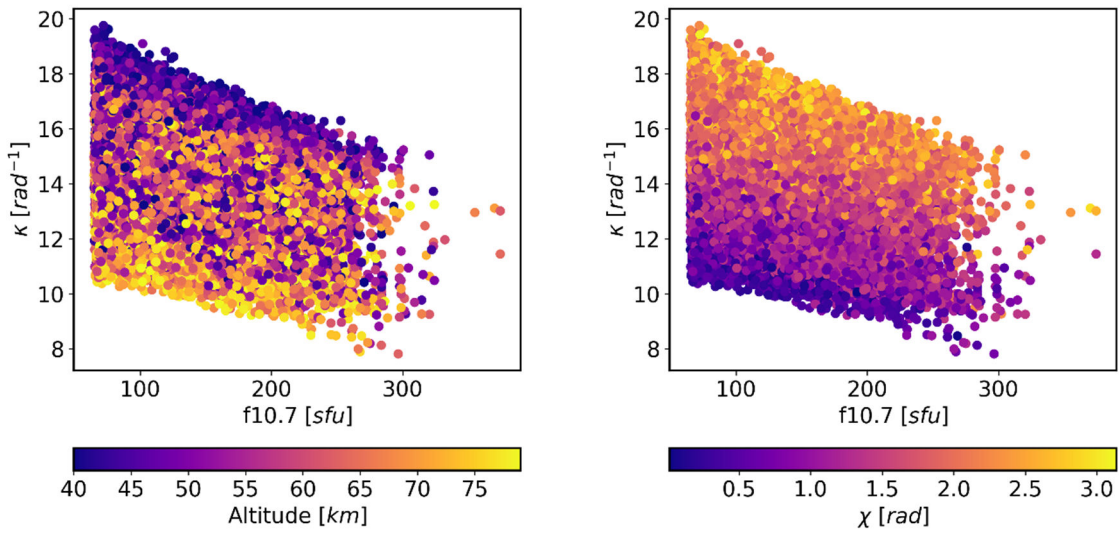
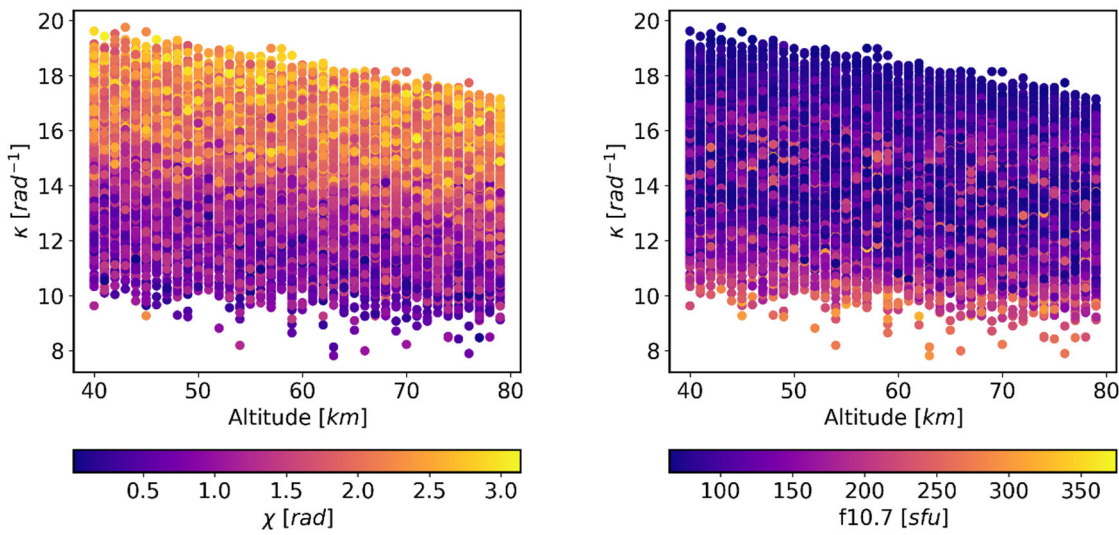


Figure 12. κ vs. f10.7, colour coded by altitude (left) and solar zenith angle (χ) (right)



5 Figure 13. κ vs. altitude, colour coded by solar zenith angle (χ) (left) and f10.7 (right)

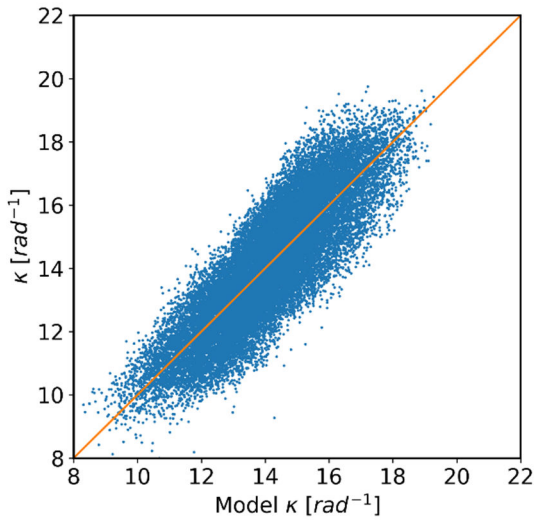
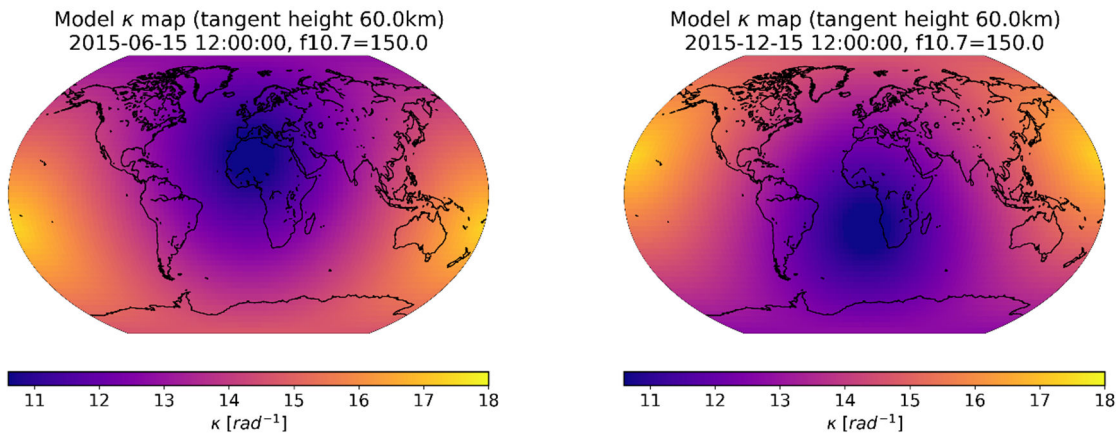


Figure 14. Scatter plot of κ estimated from NeQuick compared to modelled κ .



5 Figure 15. κ model for 12 UT, $f_{10.7}=150$, June (left) and December (right). c.f. [Figure 8](#) [Figure 8](#).

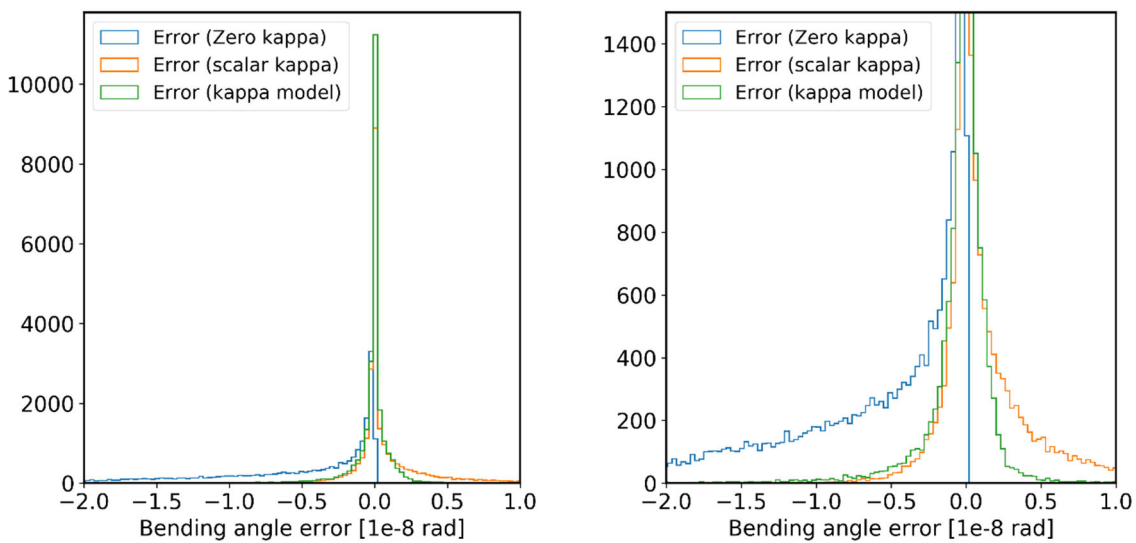


Figure 16. Histograms of globally distributed bending angle errors for zero κ , scalar κ , and modelled κ . **LeftRight**: full histogram; **leftright**: zoomed to highlight tails.

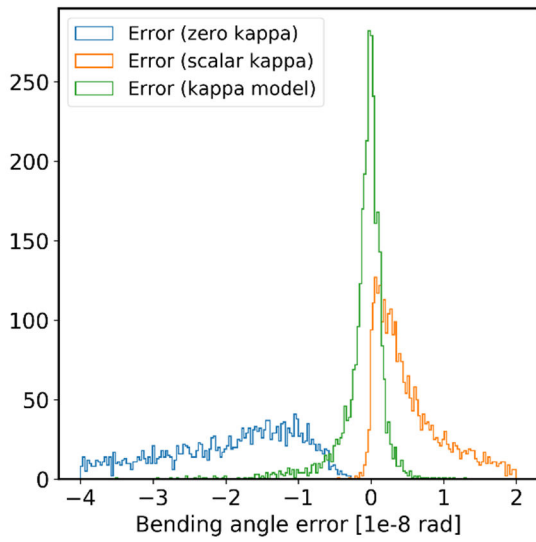
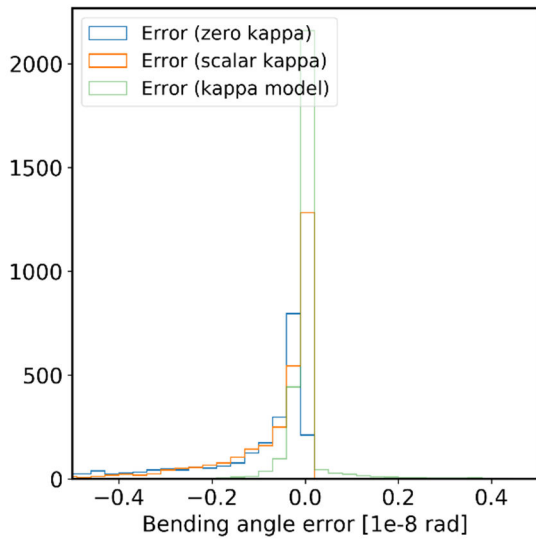


Figure 17. Histograms of day time bending angle errors for zero κ , scalar κ , and modelled κ .



5 Figure 18. Histograms of night time bending angle errors for zero κ , scalar κ , and modelled κ .

Tables

Feature	v2.0.2	UoB variant
f10.7	Clipped to: $63 < f10.7 < 193$ This is the ITU recommendation for use with the ITU ionospheric coefficients	Clipped to: $63 < f10.7$ Provides better TEC performance during high f10.7 solar cycle peaks.
Day of month	Not used	The day of month is used to linearly interpolate between two monthly coefficient files. This prevents step changes in electron density at month boundaries
hmE	Hard coded to 120 km	Hard coded to 110 km. This is a more reasonable value. However, a more sophisticated model will be implemented in future; i.e. (Chu et al. 2009).
Bottom side taper	Displays a discontinuity at 90 km that can produce artefacts in bending angle estimations	Bottomside taper added using a tanh function.

Table 1. Updates to produce the UoB variant of NeQuick.

5

Parameter	Test 1	Test 2
Latitude	50°	50°
Longitude	0°	0°
Time	12 UT	00 UT
Month	June	June
f10.7	150	150

Table 2. Test parameters for height dependence examples

Parameter	Test 1	Test 2
Latitude	-85 to 85°	-85 to 85°
Longitude	-180 to 180°	-180 to 180°
Time	12 UT	12 UT
Month	June	December
f10.7	150	150
Tangent height	60 km	60 km

Table 3. Geographic test parameters.

10

Parameter	Value
Latitude	51.5°
Longitude	-0.128°
Time	12 UT
Tangent height	60 km

Table 4. Solar cycle test parameters.

Parameter	Range
Latitude	-80 to 80°
Longitude	-180 to 180°
Time	0 to 23 UT
Day of year	1 to 365
Year	1960 to 2010
Tangent height	40 to 80 km

5 Table 5. Parameter ranges for random κ generation.

10

Parameter	Units	Estimated value	variance of the parameter estimate
a	rad ⁻¹	15.05	1.764×10^{-3}
b	rad ⁻¹ .sfu ⁻¹	-1.243×10^{-2}	1.786×10^{-8}
c	rad ⁻²	2.372	1.099×10^{-4}
e	rad ⁻¹ .km ⁻¹	-5.332×10^{-2}	3.351×10^{-7}

Table 6. Estimated model parameters and associated variances

Region	Model	Mean (rad)	Median (rad)	Standard deviation (rad)
Global	zero- κ	-1.3×10^{-8}	-4.5×10^{-9}	2.2×10^{-8}
	scal- κ (14)	1.5×10^{-9}	3.6×10^{-13}	5.4×10^{-9}
	func- κ	-2.2×10^{-10}	5.6×10^{-13}	2.0×10^{-9}
Day-time	zero- κ	-3.3×10^{-8}	-2.3×10^{-8}	2.9×10^{-8}
	scal- κ (14)	7.6×10^{-9}	4.2×10^{-9}	9.9×10^{-9}
	func- κ	-9.8×10^{-10}	-3.0×10^{-10}	3.4×10^{-9}
Night-time	zero- κ	-7.9×10^{-9}	-1.0×10^{-9}	2.3×10^{-8}
	scal- κ (14)	-7.0×10^{-10}	-1.5×10^{-10}	2.1×10^{-9}

	func- κ	1.7×10^{-10}	6.2×10^{-12}	1.9×10^{-9}
--	----------------	-----------------------	-----------------------	----------------------

Table 7. Global, day-time and night-time bending angle errors for three models